Journal of Groundwater Science and Engineering 12(2024) 78–91

Journal homepage: http://gwse.iheg.org.cn

Original Article

Formation mechanism of hydrochemical and quality evaluation of shallow groundwater in the Upper Kebir sub-basin, Northeast Algeria

Allia Zineb[1,2*], Lalaoui Meriem[1,2]

[1] *Natural Sciences and Materials Laboratory (LSNM), University Center A. Boussouf of Mila, Po Box 26 RP* 43000 *Mila, Algeria.*
[2] *Institute of Science and Technology, university Center A. Boussouf of Mila, Po Box 26 Postal Reference* 43000 *Mila, Algeria.*

Abstract: This study investigates the hydrochemical formation mechanism of shallow groundwater in the Upper Kebir upstream sub-basin (Northeastern Algeria). The objective is to evaluate water quality suitability for domestic purposes through the application of water quality index (WQI). A total of 24 water points (wells and borewells) evenly distributed in the basin were collected and analyzed in the laboratory for determining the major ions and other geochemical parameters in the groundwater. The groundwater hydrochemical types were identified as Cl–Na and Cl–HCO_3–Na, with the dominant major ions were found in the order of $Na^+ > Ca^{2+} > Mg^{2+}$ for cations, and $Cl^- > SO_4^{2-} > HCO_3^- > NO_3^-$ for anions. Results suggest that weathering, dissolution of carbonate, sulfate, salt rocks, and anthropogenic activities were the major contributors to ion content in the groundwater. The Water Quality Index (WQI) was calculated to assess the water quality of potable water. Approximately 50% of the sampled sites exhibited good water quality. However, the study highlights significant NO_3 contamination in the study area, with 50% of samples exceeding permissible limits. Therefore, effective treatment measures are crucial for the safe consumption of groundwater.

Keywords: Semi-arid; Salinization process; Nitrate; Water Quality Index; Domestic use

Received: 17 Dec 2022/ Accepted: 20 May 2023/ Published: 15 Mar 2024

Introduction

Water is an indispensable natural resource in ecosystems. It plays an vital role in sustaining life cycles and fostering socio-economic development across various different levels (Tampo et al. 2015). Clean water is essential for human communities and plays a main role in social wellbeing and human health. Maintaining water quality is a major concern for societies facing escalating water demands. This concern is particularly pronounced in regions with semi-arid or arid climates, such as Algeria, where water resources, particularly groundwater, are crucial sources of freshwater (Qasemi et al. 2018; Allia et al. 2022). Water quality depends on its composition and is susceptible to natural or anthropogenic processes. The hydrogeochemical characteristics of water reflect various influences, including lithology of watersheds and reservoirs, climate, atmospheric inputs, and human activities (Chebbah and Allia, 2014; Campo et al. 2014; Liu et al. 2019; Radfard et al. 2019; Yang et al. 2020). Poor drinking water quality gives rise to widespread acute and chronic diseases, constituting a leading cause of death in many countries (USEPA, 2007). Therefore, understanding the hydrogeochemical characteristics and mineralization process of groundwater, as well as their controlling factors, is essential for its evaluation and sustainable utilization (Yang et al. 2016). In the Upper Kebir sub-basin of NE Algeria, groundwater is an essential resource for human needs due to low and irregular rainfall. The shallow aquifer in this sub-basin faces intensive exploitation and anthropogenic pollution, leading to gradual deteri-

*Corresponding author: Allia Zineb, *E-mail address*: z.chebbah-allia@centre-univ-mila.dz

DOI: 10.26599/JGSE.2024.9280007

Zineb A, Meriem L. 2024. Formation mechanism of hydrochemical and quality evaluation of shallow groundwater in the Upper Kebir sub-basin, Northeast Algeria. Journal of Groundwater Science and Engineering, 12(1): 78-91.

oration in water quality. Chemical and physical degradations stems from agricultural, industrial practices, and domestic wastewater discharge (Abdelhamid 2016; Lalaoui et al. 2020; Allia et al. 2022). Consequently, the assessment and sustainability of groundwater resource become of utmost importance in this semi-arid region. However, the restoration the degraded water quality remains a major challenge. Establishing an effective water quality monitoring system is essential for sustainable water utilization. In this regard, this study aims to enhance the understanding of hydrogeochemical processes contributing to water salinization, thereby enabling the controlled utilization of groundwater resources for preservation and protection. This research offers a theoretical foundation to Algerian policymakers for developing suitable strategies and policies for water resource management for this region in this new century with many crises and changes. Hence, the primary objective of this research is to investigate the hydrochemical features, identify mechanisms driving water salinization, and assess the suitability of groundwater for domestic use. The study employs various techniques, major ions, and assessment criteriaspecific to this region in Algeria.

Many methodologies, including multivariate statistical techniques, hydrodynamic, hydro-chemical, and isotopic analysis, have been employed in groundwater assessment (Ganiyu et al. 2018; Marco et al. 2019). The Water Quality Index (WQI) approach has been widely used for evaluating both surface and groundwater quality. Different formulas are available for calculating WQI, each effectively transforming physiochemical parameters into easily interpretable terms for assessing drinking water quality. WQI is developed for qualitative zoning of the aquifers and determining suitable locations for drinking water wells in most research schemes (Khan, 2018). In this study, geochemical plots, ionic ratios, and WQI were used to interpret the hydrochemical data.

1 Study area

The Upper Kebir sub-basin, referred to as 10-3, is one of the seven sub-basins within the Kebir-Rhumel hydrographic basin (10). It covers the southern part of Mila district in NE Algeria (Fig. 1). Geographically, it corresponds to the upper valley of the Rhumel river, with its geographic extents spanning between latitude 36°08′–36°15′ N and longitude 6°10′–6°18′ E (Fig. 1), covering an area of 1130 km^2. Displaying a sub-circular shape, it is bounded downstream by the eastern end of the Djebel Grouz and is drained by the Oued Rhumel. Notably, the flow pattern in this sub-basin follows a temporary west-to-east direction, largely influenced by the Hammam Grouz dam situated at Oued Athménia (Lalaoui et al. 2020; Allia et al. 2022). The climate prevalent in the study area is characterized as semi-arid with a continental-type. The mean annual temperature is around 16.43°C, ranging from −2.1°C to 40.2°C. Precipitation predominantly occurs from October to May, while the dry phase prevails from June to September. The average annual rainfall is 383.10 mm/a, while the average annual evaporation, run-off and infiltration are 291.22, 67.28 and 24.60 mm/year respectively, accounting for approximately 76.01%, 17.56% and 6.42% of annual precipitation (Allia et al. 2022). The main cities in the region include Tadjennat and Chelghoum Laid. The ephemeral rivers traversing the region include Oued Rhumel, Oued El Mohari and Oued Dekri.

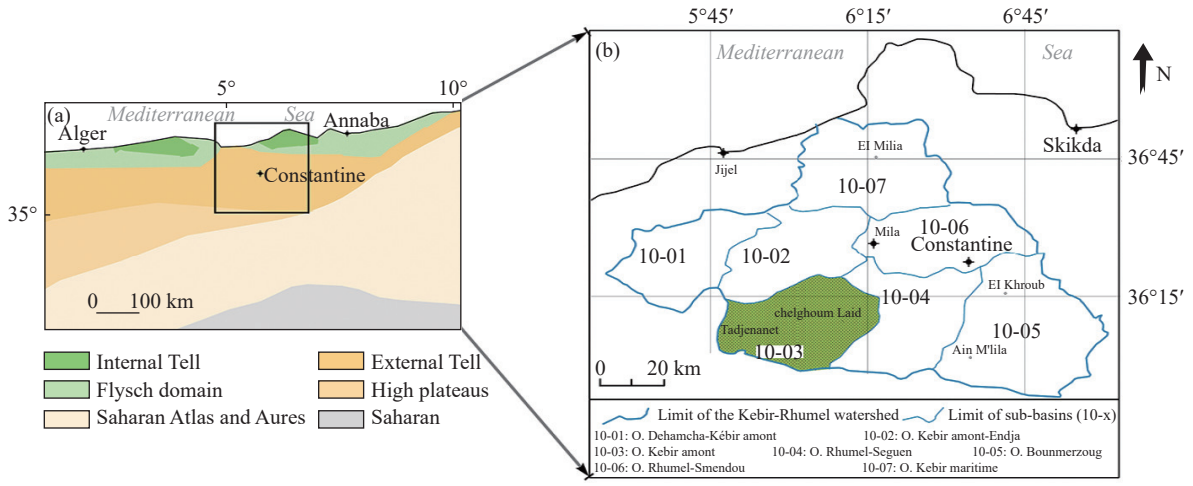

Fig. 1 A. Major geomorphologic units of North Algeria (Villa, 1980). B. Kebir Rhumel subbasins (ABH, 2014)

These rivers exhibit flow only during the rainy season. The drainage network is considerably dense, with Oued Rhumel standing out as the most prominent watercourse (ABH, 2014).

This sub-basin constitutes a syncline Mio-Plio-Quaternary plain surrounded by isolated and abrupt reliefs comprising the neritic limestone massifs and windows of Dj. Sattor and Djemila thrust sheets (Durozoy, 1960). The geology of the region is characterized by three litho-stratigraphic units (Voute, 1967; Villa, 1980). The first of these is a Lower Jurassic-Cretaceous neritic carbonate complex, comprised of limestone, dolomitic limestone and dolomite, with localized occurrences of phosphate deposits. This complex is overlain by a prevailing marly group spanning from Upper Senonian to the Paleocene period, encompassing marls and marly clays intermixed with evaporite minerals like gypsum and salts. The uppermost unit consists of heterogeneous detrital Mio-Plio-Quaternary sequences, encompassing red clays transitioning to evaporates. Extended lacustrine limestones banks, sandstones and conglomerates can also be found in this unit (Fig. 2). The plain is filled with the Mio-Plio-Quaternary deposits dominated by carbonate and silicate minerals. They are characterized by layers of red clays, occasionally mixed with gypsum, overlain by lacustrine limestone formations, conglomerates and alluvial deposits. However, these deposits have limited thickness and extent, showing rapid facies changes (Villa, 1980). The soil prevalent in this region is generally fine alluvial soil, having high agricultural fertility, particularly conducive to cereals and vegetable cultivation. However, the excessive application of chemical fertilizers in agricultural practices poses health hazards, leading to reduced crop diversity and nutrient deficiencies due to the use of various pesticides.

Hydrogeologically, the study area contains two aquifer systems. The first is a porous aquifer contained within the Mio-Plio-Quaternary formations, encompassing recent alluvium, slope deposits, polygenic glacis of Quaternary, as well as lake limestones, conglomerates, sandstones and sands containing gypsum and salt minerals. The second is a fissured and karstic aquifer contained within the Jurassic and Cretaceous carbonate formations, specifically the neritic limestones of the Upper Jurassic-Lower Cretaceous. The water balance over the past 20 years in Hammam Grouz station shows that study area experiences a deficit in water resources. The average annual rainfall stands at approximately 383.10 mm. Notably, current evapotranspiration accounts for 76.01% of precipitation, while infiltration remains remarkably low, representing only 6.42% of the total precipitation. This suggests that groundwater recharge occurs not only through effective infiltration, but also through water supply issuing from carbonate outcrops

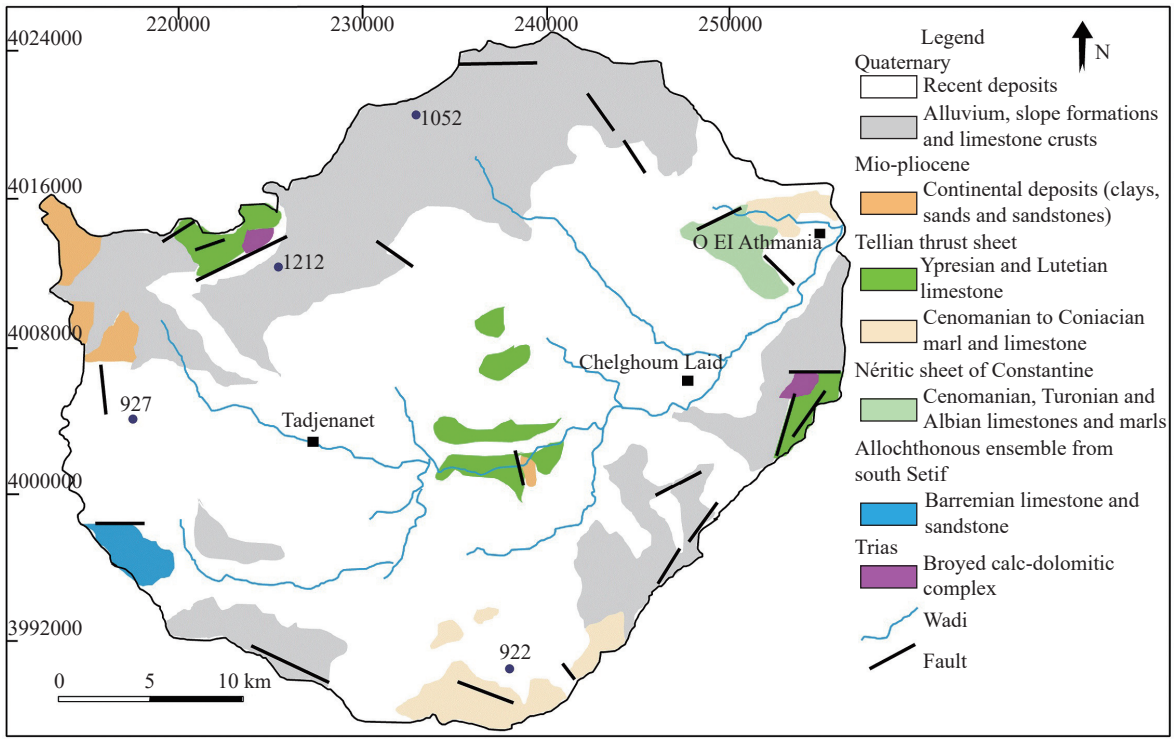

Fig. 2 Geological map of the study area, redesigned from Setif geological map at 1/200,000 (Villa, 1977)

bordering the study area (Allia et al. 2022). The studied aquifer presents a converging flow pattern, characterized by closed piezometric contour lines in a West–East direction, corresponding to the underlying bedrock morphology. These piezometric lines are very close to the West and East, signifying an average hydraulic gradient of 3%, indicating a low permeability. However, in the central and eastern parts of the study area, the pizometric lines exhibit greater spacing, reflecting a reduced hydraulic gradient of 1%. This lower gradient is attributed to the favorable hydrodynamic characteristics of the aquifer. As demonstrated by the piezometric map constructed from measurements taken in January 2020, four main flow axes of the shallow Mio-Plio-Quaternary aquifers can be identified in a NE-SW, WSW-ENE and Southwest-North-east directions. Overall, the piezometric cartography highlights a general drainage axis towards the Oued Rhumel (Fig. 3).

2 Sample collection and analytical techniques

To comprehensively assess and characterize groundwater quality and hydrochemical properties, a detailed field survey was carried out in the study area. A total of 24 evenly distributed water points in the basin were collected in February 2020 (Fig. 3). Standard methods (APHA, 2005) were employed during the collection and subsequent analysis of groundwater samples. The procedures involved acquiring groundwater samples in pre-washed 1.5-litre polyethylene bottles after pumping the wells for 5–10 minutes. Dual replicate water samples were collected for each sampling point - one bottle was acidified with HNO_3 for cation determinations, while the other was maintained unacidified for anion analyses. Subsequently, these bottles were properly sealed, correctly labeled and transported to the laboratory for further physicochemical analysis with storage maintained below 3–5°C. For all samples, temperature, pH, electrical conductivity (EC), and total dissolved solids (TDS) were determined in the field with standard field equipment using portable devices such as multi-parameter sensodirect 150. The major ions (Ca^{2+}, Mg^{2+}, CO_3^{2-} or HCO_3^-, SO_4^{2-}, Cl^- and NO_3^{2-}), total hardness (TH) and total alkalinity (TA) were analyzed in the laboratory of Natural Sciences and Materials (LSNM) of Mila University using ion photometers with tablets (Palintest photometer 7500 and Lovibond photometer MD600). Sodium ion (Na^+) was determined by flame photometer (Agilent 240/280 Series AA). In terms of geospatial context, the coordinates of sampling points were recorded using a GPS device and the Arc GIS 9.3 software was used to construct distribution maps of the various studied parameters in the study area. The Water quality index (WQI) is employed to evaluate water quality for domestic purpose. Furthermore, to verify the precision of major cations (r+) and major anions (r−) analysis, the ion balance error (IB) or standard deviation was calculated (Hounslow, 1995) , which was within acceptable limits (−2.85 and 6.42%). Finally, groundwater chemistry classification was investigated through the utilization of a trilinear Piper diagram and the ionic ratio method.

3 Results and discussion

3.1 Groundwater physical chemistry

Groundwater samples from the shallow aquifer of the Upper Kebir sub-basin were analyzed for both physical and chemical parameters (Table 1). The sampling locations are presented in Fig. 3. The physicochemical compositions of groundwater samples were statistically analyzed. Table 2 provides a summary of the minimum, maximum, mean, standard deviation, and coefficient of variation values for various parameters, alongside the guideline values set by the World Health Organization (WHO, 2008).

The pH values of the groundwater range from 6.7 to 7.85 (mean=7.15), which falls within the acceptable pH limits of 6.5–8.5, indicating that the groundwater in this area are neutral to moderately alkaline. The alkalinity, expressed as $CaCO_3$, ranges from 105 mg/L to 405 mg/L (mean: 230.54); 29.17% of samples exhibit relatively high alkalinity (> 250 mg/L). However, the majority of the samples (70.83%) have alkalinity within acceptable limits. Water temperature varies between 11.5° and 22.4°C with an average of 17.06°C. Electrical conductivity (EC) values ranges from 630 µS/cm to 5,830 µS/cm (mean: 2,549.96 µS/cm) while total dissolved solids (TDS) values cover a wide range of 509–4,223 mg/L, with a mean value of 1,686.01 mg/L. Total hardness as $CaCO_3$ ranges from 114 to 958 mg/L (mean: 440.08 mg/L), indicating that the majority of waters are hard to very hard. The dominant ions are in order of Na^+ (55.67%) > Ca^{2+} (33.87%) > Mg^{2+} (10.46%) for cations and Cl^- (48%) > SO_4^{2-} (20.6%) > HCO_3^- (23.7%) > NO_3^- (7.65%) for anions. The average concentrations of Na^+, Ca^{2+}, Mg^{2+}, Cl^-, SO_4^{2-},

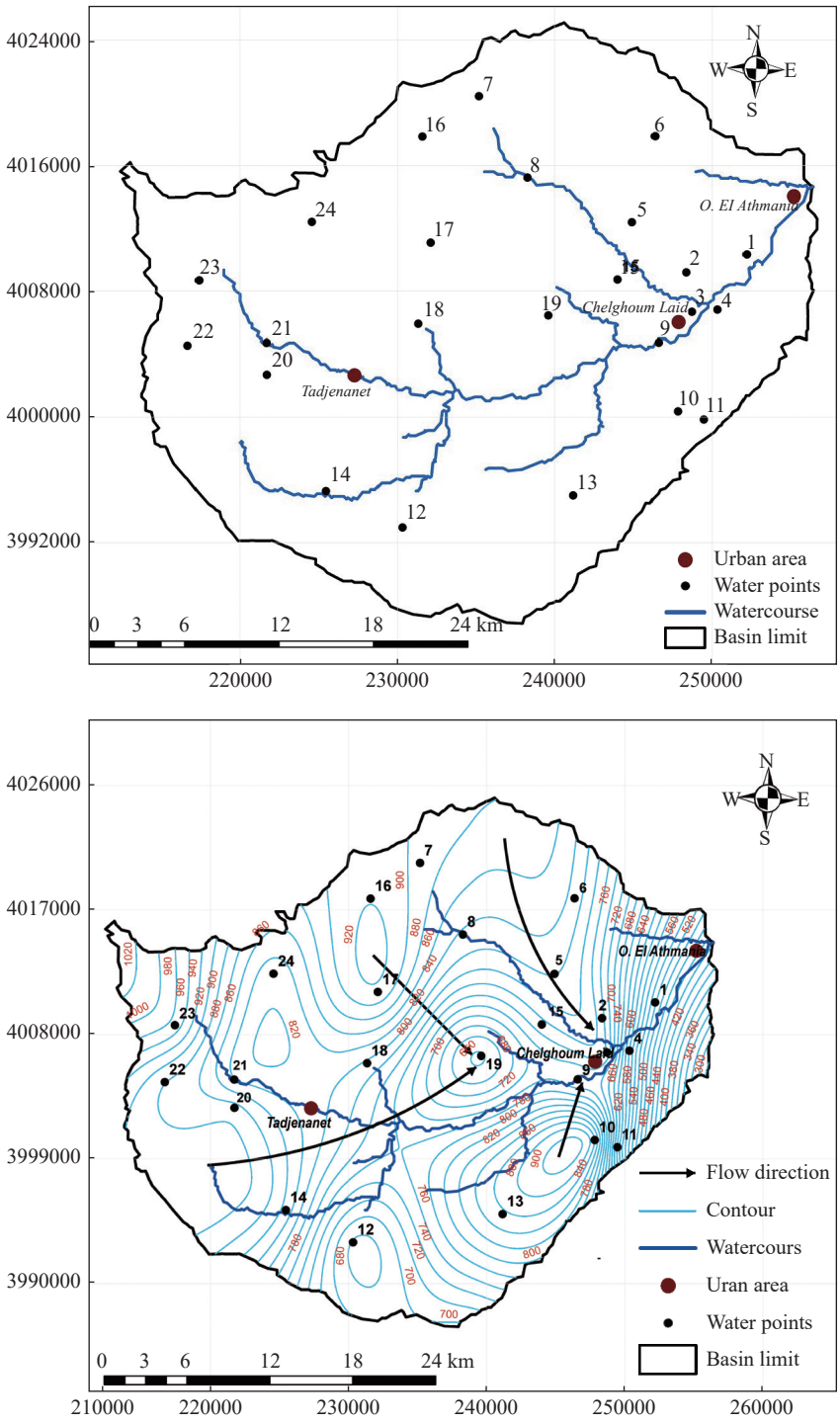

Fig. 3 Sampling location and piezometric map - January 2020- of the shallow aquifer of the upstream Kebir sub-basin (present study)

HCO_3^- and NO_3^- in groundwater were 225.13 mg/L, 141.08 mg/L, 41.75 mg/L, 375.92 mg/L, 189.08 mg/L, 183.58 mg/L and 66.54 mg/L (Table 1). Sodium and chlorine concentrations are the highest among the cations and anions, respectively. Adequate sodium intake is essential for human health, whereas excessive intake can lead to health risks such as hypertension and osteoporosis (Adimalla, 2019; Zhang et al. 2020). Regarding the WHO drinking water quality standard (2011), 12% of the groundwater samples have Na^+ concentration below the permissible limit. Both Ca^{2+} and Mg^{2+} are also essential for human health, with inadequate Ca^{2+} intake potentially leading to several diseases such as stroke, osteoporosis, and colorectal cancer. High Mg^{2+} concentrations can have a laxative effect (Zhang et al. 2020). In this study, 91.66% and 100% of the groundwater samples fall

Table 1 Physicochemical groundwater quality constituents in the Upper Kebir sub-basin

	pH	T	CE	TDS	TH	TA	O_2 dis	Ca	Mg	Na	Cl	SO_4	HCO_3	NO_3
Unit		°C	µS/cm	mg/L	mg/L	mg/L	mg/L	mg/L	mg/L	mg/L	mg/L	mg/L	mg/L	mg/L
1	7.0	15.9	1,865	1,286	494	240	0.16	115	32	182	314	76	156	28
2	7.4	14.3	1,285	1,074	280	105	0.25	94	41	154	312	79	130	35
3	7.2	20.3	1,420	1,251	477	184	0.24	143	17	208	402	86	92	36
4	7.0	22.4	2,810	1,857	470	220	1.88	186	63	241	357	86	239	37
5	7.1	15.0	4,460	2,543	320	288	0.12	126	58	257	375	87	216	37
6	7.0	20.3	960	749	450	210	0.17	154	6	227	365	120	176	37
7	7.2	19.9	1,075	744	449	312	0.16	127	42	207	375	140	225	41
8	7.1	16.5	1,609	1,163	449	342	0.06	157	67	135	379	146	284	41
9	7.0	16.3	2,900	1,869	958	376	0.29	257	62	295	432	148	292	42
10	7.1	13.0	1,200	857	372	405	0.1	186	48	208	385	157	285	48
11	7.0	18.6	702	509	268	196	0.34	95	25	213	341	157	128	53
12	7.8	13.9	630	579	292	202	0.03	95	65	210	384	157	135	54
13	7.0	15.0	2,380	1,360	852	186	0.55	105	48	291	450	158	127	62
14	7.0	16.6	885	704	292	126	0.16	128	34	205	357	162	163	68
15	7.0	11.5	4,918	3,006	491	201	8.12	114	42	265	403	163	189	68
16	7.1	16.5	2,620	1,610	373	186	3.5	84	35	242	356	169	145	82
17	7.4	15.4	5,830	4,223	412	204	2.07	136	38	214	365	178	137	82
18	7.7	17.7	3,525	2,434	343	190	6.04	143	28	238	375	186	185	92
19	7.3	19.6	5,282	3,214	538	234	5.4	203	58	239	425	198	207	94
20	7.2	17.3	4,200	2,940	433	158	0.7	129	29	259	405	213	182	95
21	7.1	21.7	1,375	1,250	365	202	0.716	139	47	228	390	241	175	108
22	6.7	17.3	2,900	1,726	114	154	0.74	133	48	224	365	385	186	114
23	7.0	15.5	4,196	2,369	570	310	0.481	189	36	229	385	428	230	115
24	7.5	18.9	2,172	1149	500	302	0.508	148	33	232	325	198	254	37

Table 2 Summary statistics of groundwater physicochemical parameters with WHO drinking water quality standards

	Min	Max	Mean	SD	CV%	WHO (2011)		Number of samples below MPL	Number of samples exceeding MPL
						DL	MPL		
pH	6.7	7.85	7.15	0.27	3.80	6.5–8.5	9.2	24	0
T (°C)	11.5	22.4	17.05	2.81	16.45	25		24	0
EC (µs/cm)	630	5,830	2,549.96	1,565.41	61.39	900	1,400	3	21
TDS (mg/L)	509	4,223	1,686.01	967.44	57.38	600	900	0	24
TH as $CaCO_3$ (mg/L)	114	958	440.08	177.04	40.23	100	500	0	24
TA as $CaCO_3$ (mg/L)	105	405	230.54	76.90	33.35	150	-	2	22
Dissolved O_2 (mg/L)	0.03	8.12	1.336	2.18	159.84	4–6	-	22	2
Ca (mg/L)	84	257	141.08	40.30	28.56	75	200	23	1
Mg (mg/L)	6	67	41.75	15.55	37.24	50	150	24	0
Na (mg/L)	135	295	225.13	36.60	16.26	-	200	2	22
Cl (mg/L)	312	450	375.92	34.23	9.10	250	600	24	0
SO_4 (mg/L)	76	486	183.58	106.23	57.87	200	500	24	0
HCO_3 (mg/L)	92	292	189.08	55.10	29.14	125	350	24	0
NO_3 (mg/L)	28	128	66.54	30.53	45.88	50	-	10	14

Min: Minimum, **Max**: Maximum, **SD**: Standard deviation, **CV%:** Coefficients of variation (%), **DL**: Desirable limits, **MPL**: Maximum permissible limits. EC, TDS, TH and TA Values are at 25°C.

within the maximum allowable limits for Ca^{2+} and Mg^{2+} (Table 2). In addition, the concentrations of HCO_3^- range from 92 mg/L to 292 mg/L. The SO_4^{2-} concentration variy from 76 mg/L to 486 mg/L. About 79.17% of groundwater samples meet the desirable limit of 200 mg/L for SO_4^{2-}, although not all samples stay within the permissible limit in the study region. Chloride concentrations range from 312 mg/L to 450 mg/L; all groundwater samples were within the upper limit (600 mg/L) but exceeded the acceptable limit (250 mg/L) for drinking water. NO_3^- concentrations vary from 28 mg/L to 128 mg/L, with 41.66% of groundwater samples within the authorized limit of 50 mg/L in the study area. Nitrogen pollution in the study area arises from intensive agriculture that use substantial amounts of fertilizers and pesticides. The elevated levels of nitrate ions at various locations can contribute to the occurrence of blue infant disease.

3.2 Hydrochemical facies and salinization process of groundwater

3.2.1 Groundwater types

The hydro-chemical types, which are determined by major ion concentrations, provide insights into the impact of chemical processes within the lithological environment and are influenced by groundwater flow patterns (Zhang et al. 2020; Freeze et al. 1979). The chemical compositions of the analyzed samples were plotted on the Piper diagram, as shown in Fig. 4. In the study area, cations of groundwater samples were primarily situated in the fields of sodium and non-dominant type. On the other hand, anions were mainly located in the field of chloride water type, except for three samples (4, 5 and 9) lacking anion dominance. Nearly all groundwater samples were positioned within the zones of sodium chloride (37.5%) and mixed type (62.5%). These hydrochemical types are largely attributed to evaporitic and dissolution of carbonate-rich material within the aquifers (Hassen et al. 2016; Allia et al. 2016).

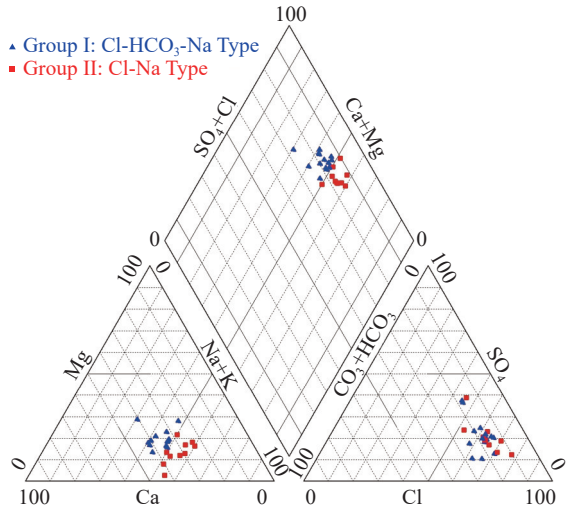

Fig. 4 Piper diagram classifying major hydrochemical facies

3.2.2 Groundwater mineralization processes

The mineralization of water occurs through weathering and water circulation within rocks and soils, where ions are leached out and dissolved in groundwater (Hassen et al. 2016). Various factors, including geological formations, water–rock interaction, ion mobility, and anthropogenic pollution, are influencing the geochemistry of groundwater. To identify the origin of groundwater mineralization in the aquifer and specify the governing processes of groundwater chemistry in the study area, several correlations and characteristic ratios between ions were employed (Long et al. 2018; Chebbah and Allia, 2014). Gibbs' diagrams were used to differentiate the impacts of these processes and represent the relationship between the lithological features of aquifers and groundwater composition (Selvakumar et al. 2017). This diagram is used to identify the origin of dissolved constituents, such as dominance of weathering, precipitation, evaporation, or combination of these influences (Gibbs, 1970). The chemical data of groundwater samples were plotted in the Gibbs diagram (TDS versus $Na^+/(Na^+ + Ca^{2+})$ and $Cl^-/(Cl^- + HCO_3^-)$). All samples fell between the field of rock weathering and the evaporation of rainfall-dominated water fields (Fig. 5), indicating that water-rock interaction, associated with the evaporation mechanism, primarily governs the dissolved components of water samples. The TDS concentrations of groundwater in the study aquifer ranged from 500 mg/L to 5,000 mg/L, implying that the water chemistry was influenced not only by rock weathering but also by evaporation and precipitation. Evaporation intensified water salinity by concentrating Na^+ and Cl^-, and a strong correlation was observed between TDS and Na^+ and Cl^-. The Hounslow ratio (Cl^-/Σanions) was utilized to conclude the significance of rock weathering and evaporation processes. Among the analyzed samples, the calculated ratios ranged from 0.437 to 0.702 and were < 0.8, indicating that rock weathering is the dominant factor (Hounslow, 1995; Ghouili et al. 2018). Groundwater in the study area is influenced by the chemical weathering of rocks and minerals which

determines the species composition of ions. This is further influenced by atmospheric precipitation, acting as a diffusion source of pollution due to its content of micro and macro-elements that impact water chemistry (Gibbs, 1970).

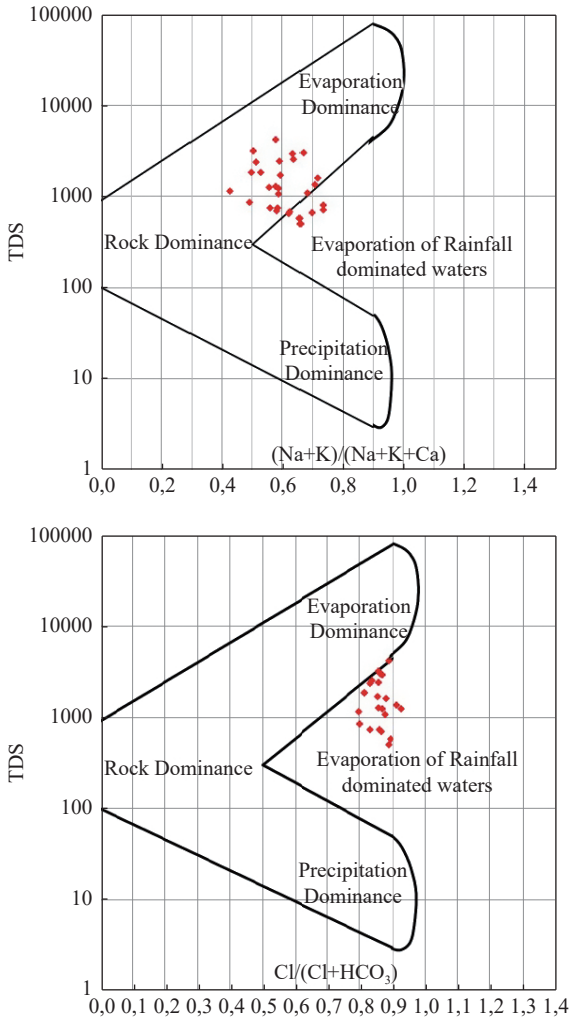

Fig. 5 Mechanisms governing groundwater chemistry in the study area (Gibbs, 1970)

The examination of the relationship between Na^+ and Cl^- concentrations has frequently been employed to identify the mechanisms behind salinity acquisition in semi-arid regions (Bouderbala et al. 2017; Fakharian and Narany, 2016). A plot of Na^+ versus Cl^- concentration (Fig. 6) reveals that a substantial portion of the points closely align with the 1:1 line, suggesting that the salinity of these points primarily originates from the dissolution of salt (halite). In fact, groundwater derived from halite dissolution tends to exhibit a Na^+/Cl^- ratio roughly equal to 1 (Bouderbala et al. 2017). However, some data points in Fig. 6 deviate from the expected 1:1 trend line, indicating that factors other than halite dissolution contribute to the presence of Na^+. In a subset of groundwater samples from the study area (31% of the samples), the Na^+/Cl^- molar ratio falls below 1 (mean value: 0.92), suggesting that an ion exchange process between water ions and the clays within the aquifers is likely responsible for the deficit of Na^+.

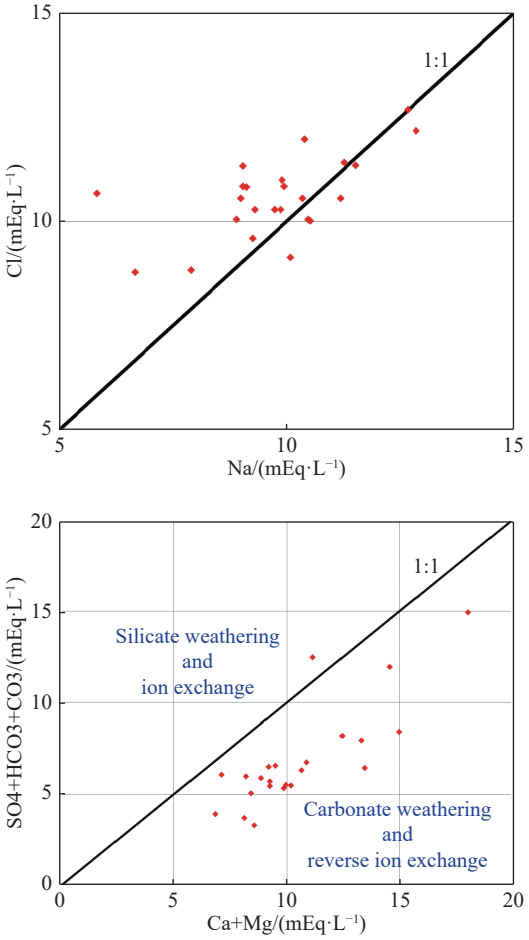

Fig. 6 Na^+ - Cl^- and $(Ca^{2+} + Mg^{2+})$ - $(SO_4^{2-} + HCO_3^- + CO_3^{2-})$ scatter diagrams for groundwater samples in the study area

In addition to Na^+ and Cl^-, the Ca^{2+}, Mg^{2+}, and HCO_3^- emerge as the dominant ions within the groundwater. These major ions in natural water sources stem from the weathering and dissolution of minerals like carbonate (calcite and dolomite evaporate (gypsum) and silicate minerals. However, the process of mineral weathering and dissolution suggests that a simple plot of $(Ca^{2+} + Mg^{2+})$ versus $(SO_4^{2-} + HCO_3^-)$ could provide insights into the relative significance of the primary minerals contributing to groundwater mineralization. The plot of analyzed samples in $(Ca^{2+} + Mg^{2+})$ versus $(SO_4^{2-} + HCO_3^-)$ diagram (Fig. 6) shows that the majority of samples are positioned above the equiline 1:1, indicating an excess of Ca^{2+} and Mg^{2+} ions and reflect the importance of the reverse ion exchange mechanism. This mechanism involves the

exchange between Na^+ and K^+ in groundwater with Ca^{2+} and Mg^{2+} in the aquifer material (Kundu et al. 2015; Allia et al. 2018; Liu et al. 2015). This finding further reinforces the Na deficit observed in the waters (Fig. 6). Furthermore, the scatter diagram of (Ca^{2+} + Mg^{2+}) versus (SO_4^{2-} + HCO_3^-) demonstrates that carbonate weathering played a crucial role in the evolution of groundwater. When calcium and magnesium dominate over bicarbonate and sulfate, it reflects that carbonate weathering is the predominant process responsible for increasing the concentration of Ca^{2+} and Mg^{2+} in groundwater.

Furthermore, the Ca^{2+}/Mg^{2+} molar ratio is used to elucidate the carbonate dissolution processes (Liu et al. 2015). When the Ca/Mg ratio is equal to 1, it suggests the occurrence of dolomite dissolution, whereas a higher ratio signifies a greater contribution from calcite. A Ca/Mg molar ratio exceeding 2 indicates the dissolution of silicate minerals, which contribute calcium and magnesium to both surface water and groundwater. In most water samples, the Ca/Mg ratio falls between 1 and 2, indicating the dissolution of calcite and dolomite (Ameen, 2019). The scatter diagram of the Ca/Mg for surface water samples in the study area reveals the dominant role of carbonates dissolution (Fig. 7). The majority of samples lie between lines 1 and 2 (Ca/Mg > 1) and below the 1:1 line (Ca/Mg = 1), indicating the dominance of calcite and dolomite weathering process. However, some samples are positioned above the 1: 2 line (Ca/Mg > 2), suggesting the influence of silicate minerals. The presence of carbonates and mineral silicates in the sediments promotes the weathering process. Similarly, if the Ca^{2+} originates from gypsum dissolution, the Ca^{2+}/SO_4^{2-} ratio would be close to 1 (Ghouili et al. 2018). However, in this study, the Ca^{2+}/SO_4^{2-} ratio significantly exceeds 1 (Fig. 7), suggesting that the excess Ca^{2+} may be derived from carbonate dissolution, with a minor contribution from silicate minerals.

Finally, the presence of the sodium-chloride water type in the study area can be attributed to several factors, including the sluggish movement of groundwater, ion exchange processes, prolonged interaction between water and rock formation, rock types, and the potential influence of irrigation return water, where agricultural practices involves excessive soil fertilization.

3.3 Water Quality Index (WQI)

The suitability of water for human consumption is directly related to various physicochemical parameters and their concentrations. This evaluation can be performed by comparing the values of these parameters in the analyzed water with drinking water standards or by using the Water Quality Index (WQI). The assessment of drinking water quality for the examined samples was conducted using water quality index (WQI) in accordance with WHO standards. The WQI, widely utilized, is a comprehensive numerical rating that reflects the impact of diverse water quality parameters on the overall water quality for specific purposes (Ameen, 2019). This method is highly valuable for quantitatively describing the overall status of water quality using a single term, which simplifies the interpretation of enormous amounts of physicochemical data. The WQI effectively illustrates the complex influence of numerous water quality parameters and provides a quantified representation of water quality information, beneficial for both decision-makers and the general public. This tool serves as an essential method to interpret the general status of water quality in a simple and comprehensible manner (Horton, 1965; Tyagi et al. 2020). The computation of WQI is based on the drinking water quality standards recommended by the World Health Organization (WHO, 2011). Fifteen (15) parameters are involved in the WQI calculation, using the weighted arithmetic index method (Shah et al. 2017).

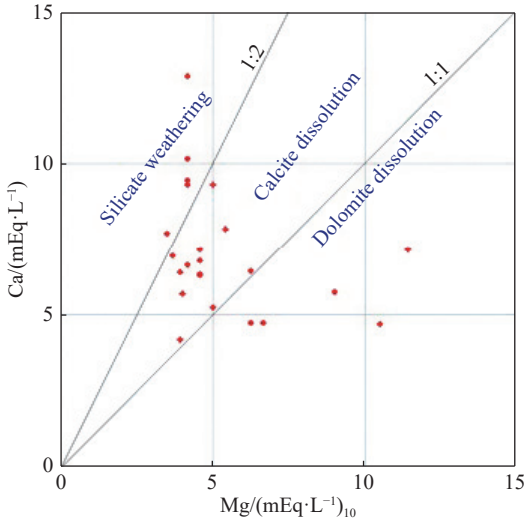

Fig. 7 Mg^{2+} - Ca^{2+} and SO_4^{2-} - Ca^{2+} scatter diagrams for groundwater in the study area

The physicochemical parameters were assigned weights (W_i) based on their significant influence on overall drinking water quality, following the criteria recommended by WHO in 2017. According to the potential influence on human health, each criterion is assigned a specific weight (W_i), ranging

from 1 (indicating the lowest impact on water quality) to 5 (indicating the highest impact) (Perera et al. 2022).

The relative weightage (W_i) is calculated using Equation 1:

$$W_i = w_i / \Sigma w_i \quad (1)$$

Where: W_i = relative weight, w_i = the weight of each parameter, and n = number of parameters considered for the calculation of WQI. The calculated W_i values for each parameter are presented in Table 4.

The quality rating scale (Q_i) for each parameter is determined based on their compliance with the drinking water quality standards (S_i) established by WHO guidelines (WHO, 2011). The quality rating scale for each parameter is determined using Equation 2:

$$Q_i = (C_i / S_i) \times 100 \quad (2)$$

Where: C_i = concentration of each chemical parameter in each sample (mg/L) and S_i = drinking water standards specified by WHO for each chemical parameter (mg/L).

The subindex value for each chemical parameter is calculated using Equation 3:

$$SI_i = W_i \times Q_i \quad (3)$$

The aggregated WQI is calculated using Equation 4:

$$WQI = \Sigma SI_i \quad (4)$$

The computed WQI scores for all groundwater samples were then categorized into one of five water quality classes (Kachroud et al. 2020, Maskooni et al. 2020), as indicated in Table 3.

The WQI of the groundwater samples was evaluated using ten water quality parameters. Each parameter was assigned a weight (W_i) based on its significant influence on overall drinking water quality, in accordance with WHO (2011) standards (S_i) for each parameter (Table 3). Fig. 8 demonstrates that around 45.83% of the samples exhibited a good WQI, indicating suitability for potable use, while 58.33% of the samples fell into the poor category. Samples with elevated concentration of EC, Cl^-, Na^+ and NO_3^{2-} exhibit higher WQI (> 100) and are considered unsuitable for drinking purposes.

As presented in Fig. 8, water quality varied from good to poor quality type across the study area. The good water quality was mainly observed in the peripheral parts of the sub-basin, whereas poor water quality was scattered in the northwest and central sectors. The elevated WQI values observed in the study area were primarily attributed to high values of pH, TDS, EC, Na^+, SO_4^{2-}, Cl^-, and total

Table 3 Classification of water quality

Ranking	WQI Value	Explanation
<50	Excellent water	Good for human health
50–100	Good water	Suitable for human consumption
100–200	Poor water	Water in poor condition
200–300	Very poor water	Needs special attention before use
>300	Unsuitable for drinking	Requires too much attention

Table 4 WQI Computation of groundwater in the study area

	S_i	w_i	W_i	C_i (Mean values)	q_i	SI
pH	8.5	3	0.097	7.15	84.14	8.16
T (°C)	25	4	0.129	17.05	68.24	8.80
EC (µs / cm)	1500	3	0.097	2,549.96	170.00	16.49
Ca (mg/L)	200	2	0.065	141.08	70.54	4.59
Mg (mg/L)	150	2	0.065	41.75	27.83	1.81
Na (mg/L)	200	2	0.065	225.13	112.56	7.32
Cl (mg/L)	250	4	0.128	375.92	126.06	16.14
SO_4 (mg/L)	250	3	0.097	183.58	73.43	4.12
HCO_3 (mg/L)	125	3	0.097	189.08	150.37	14.59
NO_3 (mg/L)	50	5	0.160	66.54	133.08	21.29
		$\Sigma w_i = 31$	1			

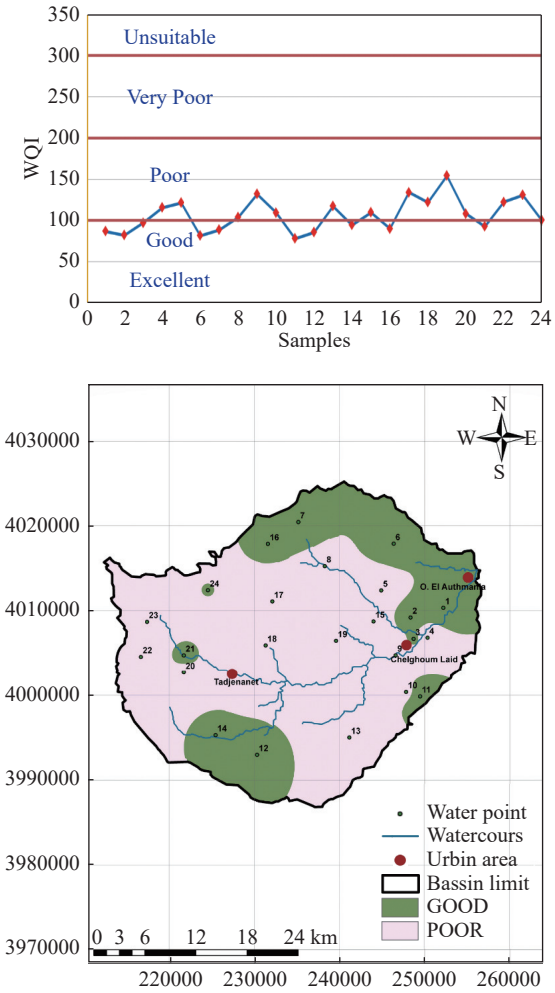

Fig. 8 Values and distribution map of the WQI of groundwater in the study area

hardness (TH). Notably, strong correlation coefficients among these values were also evident in the current study (Table 2 and Table 4).

4 Conclusion

The primary objective of this study was to investigate the mineralization mechanisms and assess the suitability of groundwater for domestic consumption in the shallow aquifer of the Upper Kebir subbasin in NE Algeria. The study identified two distinct types of water chemistry in the study area: Na-Cl and Cl-HCO_3-Na. By combining analyses of Gibbs diagram, ion relationships , and ion ratios to analyze the origin of major groundwater ions, it was determined that the chemical composition of groundwater in the study area is primarily influenced by processes like rock weathering and dissolution (including carbonate, sulfate and salt rocks), along with anthropogenic activities. The application of Water Quality Index (WQI) methodology enabled the classification of various water quality class and GIS was used to visually depict their spatial distribution within the study area. The results revealed that merely 45.85% of the analyzed samples fall into the category of "excellent to good" water quality, making them suitable for drinking purposes. This investigation highlights the influence of diverse factors and/or mechanisms on water mineralization. The insights gained from this study could provide a foundational understanding for the protection and management of groundwater quality in this semi-arid area, where comprehensive treatment systems might be lacking.

References

Abdelhamid K. 2016. Caractérisation des paramètres hydrodynamiques de l'aquifère deTadjnant –Chelghoum Laid et impact de la pollution des eaux desurface sur les eaux souterraines. Thèse Doc. Es. Sci., Univ. Batna2: Algérie: 162.

ABH. 2014. Le bassin du Khébir Rhumel. Cahiers de l'agence 15 : Alger.

Adimalla N, Qian H. 2019. Groundwater quality evaluation using water quality index (WQI) for drinking purposes and human health risk (HHR) assessment in an agricultural region of Nanganur, South India. Ecotoxicology and Environmental Safety, 176: 153−161. DOI：10.1016/j.ecoenv.2019.03.066.

Allia Z, Lalaoui M, Chebbah M. 2022. Hydrochemical assessment for the suitability of drinking and irrigation use of surface water in Grouz Dam Basin, Northeast Algeria. Sustainable Water Resources Management, 8(3): 88. DOI：10.1007/s40899-022-00663-8.

Allia Z, Chebbah M, Ouamane A. 2018. Analyse et évaluation de la qualité des eaux du système aquifère mio-pliocène dans le Zab Chergui, Bas Sahara Septentrional. Courrier du Savoir, univ Biskra, Algérie, 26: 235−244

Ameen HA. 2019. Spring water quality assessment using water quality index in villages of Barwari Bala, Duhok, Kurdistan Region, Iraq. Applied Water Science, 9(8): 176. DOI：10.1007/s13201-019-1080-z.

APHA. 2005. Standard methods for examination

of water and wastewater 21st ed. American Public Health Association, Washington D. C.

Bouderbala A, Gharbi BY. 2017. Hydrogeochemical characterization and groundwater quality assessment in the intensive agricultural zone of the Upper Cheliff plain, Algeria. Environmental Earth Sciences, 76(21): 744. DOI：10.1007/s12665-017-7067-x.

Campo M, Esteller MV, Exposito J. et al. 2014. Impacts of urbanization on groundwater hydrodynamics and hydrochemistry of the Toluca Valley aquifer (Mexico). Environmental Monitoring and Assessment, 186: 2979−2999. DOI：10.1007/s10661-013-3595-3.

Chebbah M, Allia Z. 2014. Geochemistry and hydrogeochemical process of groundwater in arid region: A case study of the water table in the Souf Valley (Low Septentrional Sahara, Algeria). African Journal of Geo-Science Research, 2(3): 23−30.

Durozoy G. 1960. Etude géologique de la région de Châteaudun du Rhumel, publ. Serv. Carte Géol. Algérie, Nlle sér. 22, Alger.

Fakharian K, Narany TS. 2016. Multidisciplinary approach to evaluate groundwater salinity in Saveh Plain, Iran. Environmental Earth Sciences, 75(7): 624. DOI：10.1007/s12665-015-5104-1..

Freeze RA, Cherry JA. 1979. Groundwater, Prentice-Hall, Inc. Englewood Cliffs, New Jersey 07632, United States of America. p 589.

Ganiyu SA, Badmus BS, Olurin OT, et al. 2018. Evaluation of seasonal variation of water quality using multivariate statistical analysis and irrigation parameter indices in Ajakanga area, Ibadan, Nigeria. Applied Water Science, 8(1): 35. DOI：10.1007/s13201-018-0677-y.

Ghouili N, Hamzaoui-Azaza F, Zammouri M, et al. 2018. Groundwater quality assessment of the Takelsa phreatic aquifer (Northeastern Tunisia) using geochemical and statistical methods: Implications for aquifer management and end-users. Environmental Science and Pollution Research, 25(36): 36306−36327. DOI：10.1007/s11356-018-3473-1.

Gibbs RJ. 1970. Mechanisms controlling world water chemistry. Science, 170(3962): 1088−1090. DOI：10.1126/science.170.3962.1088.

Hassen I, Hamzaoui-Azaza F, Bouhlila R. 2016. Application of multivariate statistical analysis and hydrochemical and isotopic investigations for evaluation of groundwater quality and its suitability for drinking and agriculture purposes: Case of Oum Ali-Thelepte aquifer, central Tunisia. Environmental Monitoring and Assessment, 188(3): 135. DOI：10.1007/s10661-016-5124-7.

Horton RK. 1965. An index number system for rating water quality. Journal of the Water Pollution Control Federation. 37(3): 300–306.

Hounslow AW. 1995. Water quality data analysis and interpretation. CRC Press, Boca Raton, CRC Press LLC.

Kachroud M, Trolard F, Kefi M, et al. 2019. Water quality indices: Challenges and application limits in the literature. Water, 11(2): 361. DOI：10.3390/w1020361.

Khan A, Qureshi FR. 2018. Groundwater quality assessment through water quality index (WQI) in New Karachi Town, Karachi, Pakistan. Asian Journal Water Environment Pollution, 15(1): 41−46. DOI：10.3233/AJW-180004.

Kundu A, Kanti Nag, S. 2015. Delineation of groundwater quality for drinking and irrigation purposes: A case study of chhatna block, Bankura District, West Bengal. International Journal of Water Resources Development, 3(1): 5−23.

Lalaoui M, Allia Z, Chebbah M. 2020. Hydrogeochemical processes and suitability assessment of surface water in the Grouz Dam Basin, northeast Algeria. Journal of Fundamental and Applied Sciences, 12(3): 1452−1474. DOI：10.4314/jfas.v12i3.29.

Liu F, Song X, Yang L, et al. 2015. Identifying the origin and geochemical evolution of groundwater using hydrochemistry and stable isotopes in the Subei Lake Basin, Ordos energy base, Northwestern China. Hydrology and Earth System Sciences, 19(1): 551−565. DOI：10.5194/hess-19-551-2015.

Liu JT, Feng JG, Gao ZJ, et al. 2019. Hydrochemi-

cal characteristics and quality assessment of groundwater for drinking and irrigation purposes in the Futuan River Basin, China. Arabian Journal of Geosciences, 12(18): 560. DOI：10.1007/s12517-019-4732-2.

Long DT, Pearson AL, Voice TC, et al. 2018. Influence of rainy season and land use on drinking water quality in a karst landscape, State of Yucatán, Mexico. Applied Geochemistry, 98(11): 265−277. DOI：10.1016/j.apgeochem.2018.09.020.

Marco R, Tullia B, Elisa S. et al. 2019. The effects of irrigation on groundwater quality and quantity in a human-modified hydro-system: The Oglio River Basin, Po Plain, northern Italy. Science of the Total Environment, 672: 342−356. DOI：10.1016/j.scitotenv.2019.03.427.

Maskooni EK, Naseri-Rad M, Berndtsson R. 2020. Use of heavy metal content and modified Water Quality Index to assess groundwater quality in a semiarid area. Water Quality and Contamination, 12(1115). DOI：10.3390/w12041115.

Perera TANT, Herath HMMSD, Piyadasa RUK, et al. 2022. Spatial and physicochemical assessment of groundwater quality in the urban coastal region of Sri Lanka. Environmental Science and Pollution Research, 29(11): 16250−16264. DOI：10.1007/s11356-021-16911-x.

Qasemi M, Farhang M, Biglari H, et al. 2018. Health risk assessments due to nitrate levels in drinking water in villages of Azadshahr, northeastern Iran. Environmental Earth Sciences, 77(23): 782. DOI：10.1007/s12665-018-7973-6.

RadFard M, Seif M, Ghazizadeh Hashemi AH, et al. 2019. Protocol for the estimation of drinking water quality index (DWQI) in water resources: Artificial neural network (ANFIS) and Arc-Gis. MethodsX, 6: 1021−1029. DOI：10.1016/j.mex.2019.04.027.

Selvakumar S, Chandrasekar N, Kumar G. 2017. Hydrogeochemical characteristics and groundwater contamination in the rapid urban development areas of Coimbatore, India. Water Resources and Industry, 17: 26−33. DOI：10.1016/j.wri.2017.02.002.

Shah KA, Joshi GS. 2017. Evaluation of water quality index for River Sabarmati, Gujarat, India. Applied Water Science, 7(3): 1349−1358. DOI：10.1007/s13201-015-0318-7.

Tampo L, Gnazou DTM, Kodom T, et al. 2015 Suitability of groundwater and surface water for drinking and irrigation purpose in Zio River Basin (Togo). Journal of Scientific Research of the University of Lomé (Togo), 17(3): 35−51.

Tyagi S, Sharma B, Singh P, et al. 2020. Water quality assessment in terms of water quality index. American Journal of Water Resources, 1(3): 34−38. DOI：10.12691/ajwr-1-3-3.

Villa JM. 1977. Carte géologique de Sétif au 1/200 000. Publication SONATRACH, Algérie : 98. (In French)

Villa JM. 1980. La chaîne alpine d'Algérie orientale et des confins algéro-tunisiens. Thèse Docteur ès Sciences. Paris VI, France: 665. (In French)

Voute C. 1967. Essais de synthèse de l'histoire géologique des environs d'Ain Fakroune, Ain Babouche, et des environs limitrophes. Publ. Serv. Carte géol. Algérie, Nlle Série, 2 t. Essais de synthèse de l'histoire géologique des environs d'Ain Fakroune, Ain Babouche, et des environs limitrophes. Publ. Serv. Carte géol. Algérie, Nlle Série: 192. (In French)

WHO 2008. World Health Organisation Guidelines for Drinking Water Quality, Third Editions. 20 Avenue Appia, 1211 Geneva 1227, Switzerland.

WHO. 2011 World Health Organization Guidelines for Drinking Water Quality, 4rd editions. Incorporating the First and Second ADDENDA, Vol 1. Recommendation, Geneva.

WHO. 2017. World Health Organization Guidelines for Drinking-water quality, 4rd editions. Incorporating the First addendum, Geneva.

Yang L, Zhang YP, Wen XR, et al. 2020. Characteristics of groundwater and urban emergency water sources optimazation in Luoyang, China. Journal of Groundwater

Science and Engineering, 8(3): 298−304. DOI：10.19637/j.cnki.2305-7068.2020.03.010.

Yang QC, Li ZJ, Ma HY, et al. 2016. Identification of the hydrogeochemical processes and assessment of groundwater quality using classic integrated geochemical methods in the Southeastern part of Ordos Basin, China. Environmental Pollution, 218: 879−888. DOI：10.1016/j.envpol.2016.08.017.

Zhang QY, Xu PP, Qian H. 2020. Groundwater quality assessment using improved water quality index (WQI) and human health risk (HHR) evaluation in a semi-arid region of northwest China. Exposure and Health, 12(3): 487−500. DOI：10.1007/s12403-020-00345-w.